Figure 1. Clinical Appearance of FEVR
Fundus photograph of the right eye of the proband from family 1 (individual III:2 in Figure S1), showing the retinal vessels drawn up in a retinal fold that is obscuring the macula.

that they had a phenotype similar to that of the FEVR mouse models.[24] Prompted by this finding, they showed that Tspan12 is a component of the Norrin-LRP5-FZD4 signaling complex and enhances the level of Norrin-β-catenin signaling but not Wnt-β-catenin signaling.[24]

These results suggest that *TSPAN12* (MIM 613138) on chromosome 7q31.31 is an excellent candidate for involvement in FEVR, and we therefore screened this gene in a panel of 70 FEVR patients. Informed consent was obtained from all subjects tested, and ethical approval was obtained from the Leeds Teaching Hospitals Trust Research Ethics Committee. We designed primers (see Supplemental Data, available online) and screened all seven coding exons and flanking intronic sequences by direct sequencing, using standard protocols. In total, we discovered seven heterozygous *TSPAN12* mutations not present in controls (Figure 2).

We first identified a 7 bp insertion in exon 4, c.218_219insGCTCTTT, in an Australian family of European descent (family 1). This mutation causes a frameshift resulting in 45 incorrect amino acids after codon 72, followed by premature termination at codon 118 (p.F73LfsX118). The female proband in this family shows macula ectopia, with a large retinal fold across the fovea of her right eye and fibrovascular changes in the temporal periphery of her left eye (Figure 1). Her asymptomatic father also carries the mutation and has bilateral peripheral retinal pigmentary disturbances that are reminiscent of the bone-spicule pattern more commonly associated with retinitis pigmentosa (Supplemental Data). This unusual finding was interpreted as being old exudative retinal detachments that have spontaneously resolved. The proband's asymptomatic brother was also found to carry the mutation, but fundus examination revealed no signs of disease. However, he was only 10 yrs old when examined, and fundus fluorescein angiography was not performed, so a mild phenotype could not be excluded.[25]

In a second family, originating from Japan (family 2), we identified a nonsense mutation in exon 6, c.419T>A, segregating with the disease. This mutation causes the TSPAN12 protein to be truncated from 305 amino acids to 139 (p.L140X). The female proband was diagnosed in infancy with bilateral retinal folds. Her mutation-carrying father is asymptomatic but has areas of avascularity and abnormal vessels in the peripheral retina.

The third mutation identified was a nonsense change in exon 3, c.68T>G, in an isolated FEVR patient from the USA. This mutation is predicted to encode a significantly truncated protein of only 22 amino acids (p.L23X). The patient is a 6-yr-old white female with bilateral retinal folds and unilateral, persistent hyperplastic primary vitreous (persistent fetal vasculature). No DNA was available from other family members, but none reported eye problems.

The fourth mutation identified was a 5 bp deletion at the end of intron 5, c.361-1_361-5delACCAG, in an isolated FEVR patient from the UK. This mutation removes the splice acceptor site including the consensus AG. The precise effect of this mutation has not been determined because RNA was unavailable. However, possible outcomes include the deletion of exon 6 (which would result in the in-frame deletion of the 36 amino acids encoded by exon 6), the retention of intron 5 (which would result in a frameshift and premature-termination codon, p.P122SfsX125), or the activation of an unknown cryptic splice site. The white female patient had no family history of the disease and was not diagnosed herself until the fifth decade of life. She has bilateral temporal retinal avascularity and associated areas of exudation visible with fundus fluorescein angiography. In addition, both eyes show traction of the retinal vasculature at the posterior pole.

We identified a second putative splice-site mutation at the start of intron 4, c.149+3A>G, in an American family originating from Europe (family 3). No RNA was available for testing of the pathogenic nature of this DNA change, but it was excluded from over 500 ethnically matched control chromosomes. This mutation is in the splice donor site at the end of exon 3, and the most common outcome for these types of mutations is the deletion of the preceding exon (which would result in a frameshift and a premature-termination codon, p.L23GfsX88). The proband of the family is an 8-yr-old female with bilateral retinal folds affecting the macula. Her mutation-carrying mother is asymptomatic but was noted to have bilateral peripheral retinal pigment pallor, possibly indicating avascularity. A maternal cousin, who also carries the mutation, was diagnosed with a unilateral retinal fold in infancy. Her mutation-carrying mother (proband's maternal aunt) showed no signs of FEVR, although she was not examined by fundus fluorescein angiography. A maternal uncle was reported to have undergone a spontaneous retinal

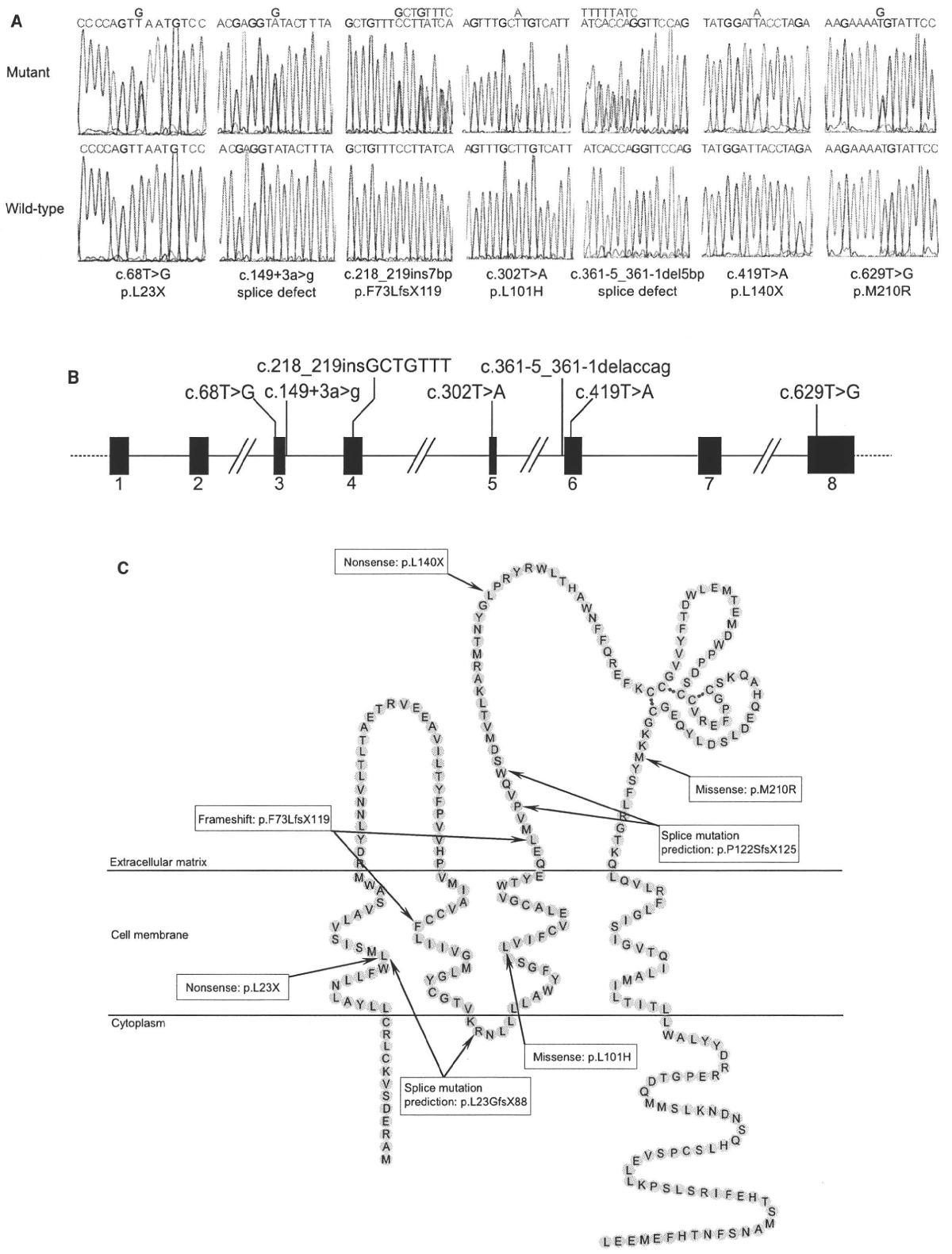

Figure 2. FEVR Is Caused by Mutations in *TSPAN12*

(A) Sequence traces of the seven mutations identified and the corresponding wild-type alleles.

(B) Schematic diagram of *TSPAN12*, showing the locations of the mutations.

(C) Schematic diagram of the TSPAN12 protein, showing the location of the mutations within the protein domains. The locations of the transmembrane domains were obtained from Kovalenko et al., 2005.[32] The intramolecular disulfide bonds crucial for the correct folding of large extracellular loop are indicated by red dots. Because we were unable to assess the actual consequences of the two splicing mutations, only predicted protein outcomes are shown.

detachment at age 27, but no DNA was available for checking whether he carried the mutation.

The remaining two mutations were missense changes. We identified p.L101H (c.302T>A) in exon 5 in a white British family (family 4). The male proband and his father both carried the mutation and showed classic signs of FEVR, with the proband being severe and the father mild. We identified p.M210R (c.629T > G) in exon 8 in a white Australian male patient with bilateral retinal detachments. This patient had no history of prematurity and presented at 5 yrs of age with a divergent squint. Upon examination he was found to have bilateral macular traction and exudates in the temporal retina. DNA was not available for family members, but there is no reported family history of disease. To exclude the possibility that these changes were common polymorphisms, we screened 200 ethnically matched control individuals (400 chromosomes) for each of these changes.[26] We also checked each of the mutated amino acids for conservation within orthologs of TSPAN12 (Figure 3). Both p.L101H and p.M210R are changes to highly conserved residues, and both mutations have negative Blosum62 scores (−3 and −1, respectively).[27] Although these results suggest that these missense changes are indeed pathogenic, without further examination by means of a functional assay, we are unable to categorically prove that they are disease-causing mutations.

All types of mutations were identified (insertion, deletion, nonsense, missense, and splicing), and at least four of these are predicted to lead to transcripts with premature-termination codons that are likely to be targeted by nonsense-mediated decay. Furthermore, there was no difference in phenotype between the patients with truncating mutations and those with missense changes. We therefore propose that haploinsufficency of TSPAN12 is the cause of FEVR. From the clinical phenotypes observed in the patients with *TSPAN12* mutations, it is clear that there is no correlation between particular mutations or mutation types and phenotype for this form of FEVR. The eye phenotypes vary in a manner similar to those reported in *FZD4*, *NDP*, and *LRP5* mutation carriers. *LRP5* mutation carriers therefore remain the only subset of FEVR patients that can be clinically distinguished by the presence of low bone-mass density.[5,9,28]

TSPAN12 is a member of the tetraspanin superfamily, of which there are 33 members in humans.[29] Tetraspanins contain four transmembrane domains with both the N and C termini located in the cytoplasm. The transmembrane domains are linked by three loops: a small extracellular loop, a large extracellular loop, and a tiny inner loop (Figure 2C). Members of this protein family are characterized by their ability to interact laterally with other tetraspanins and interacting proteins, thereby facilitating the production of large multimolecular membrane complexes, also called tetraspanin webs.[30] Through a number of cell-based assays and genetic interaction screens, Junge and colleagues showed that TSPAN12 associates with the Norrin-FZD4-LRP5 signaling complex and that this association

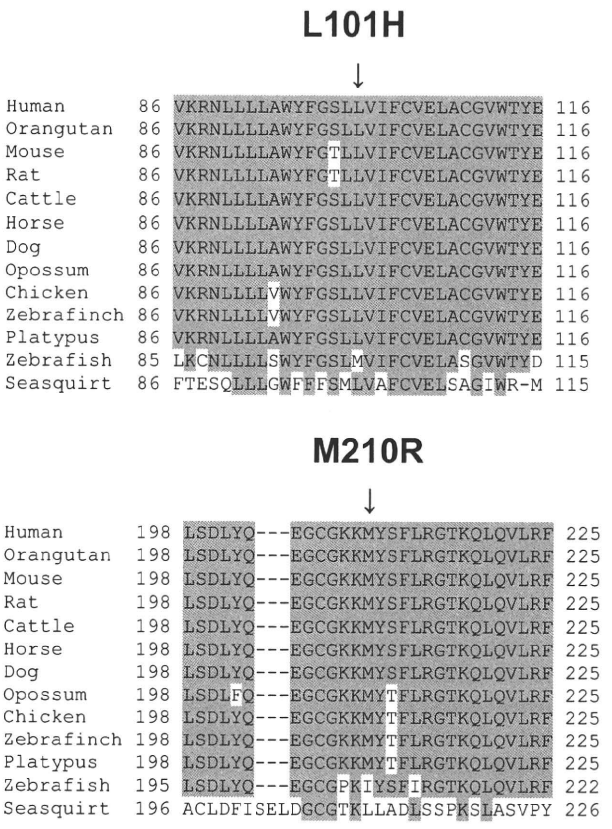

Figure 3. Protein Sequence Alignment of Human TSPAN12 with Its Orthologs

Alignments were calculated with ClustalW.[33] Accession numbers: Human, O95859; Orangutan, Q5R8B5; Mouse, AAH68240; Rat, Q569A2; Cattle, Q29RH7; Horse, XP_001502093; Dog, XP_855095; Opossum, XP_001364876; Chicken, XP_416007; Zebrafinch, XP_002192381; Platypus, XP_001516347; Zebrafish, NP_957446; Seasquirt Tspan,12 XP_002123238. Only 30 amino acid residues surrounding each mutation are shown. Conserved amino acid residues are highlighted. The positions of the missense mutations p.L101H and p.M210R are indicated.

results in an increased level of Norrin-β-catenin signaling, assayed with the Topflash reporter assay. Using the same assay, they also showed that overexpression of TSPAN12 could rescue the reduction in β-catenin signaling observed with either mutant Norrin or mutant FZD4 proteins (p.C95R and p.M147V, respectively). On the basis of these results, the authors hypothesize that Norrin and TSPAN12 cooperatively induce the multimerization of the FZD4-LRP5 complex to induce β-catenin signaling.[24] It is interesting to note that both of the missense mutations identified in this study are located in regions that are predicted to play a role in tetraspanin homo- and heterodimerization, indicating that they may disrupt the multimerization of TSPAN12.[31] The identification of additional *TSPAN12* mutations in the future will enable a more detailed analysis of the domains of TSPAN12 that are functionally important in Norrin-β-catenin signaling.

In summary, we have shown that heterozygous mutations in *TSPAN12* can cause autosomal-dominant FEVR.

Mutations in this gene accounted for 10% of FEVR cases in our patient series, although this figure is inflated because the majority of these patients had already been excluded as carrying mutations in *FZD4*, *LRP5*, and *NDP*. This result provides further evidence of significant genetic heterogeneity in FEVR and indicates that other FEVR genes remain to be found. In addition, this result confirms the importance of the Norrin-β-catenin signaling pathway in the development of the retinal vasculature and suggests that the remaining FEVR genes will also be part of this new signaling pathway.

Supplemental Data

Supplemental Data include one figure and one table and can be found with this article online at http://www.ajhg.org.

Acknowledgments

We thank the FEVR families for their help in this study. The financial support of The Royal Society (C.T. is a Royal Society University Research Fellow) and the Wellcome Trust (080313/Z/06) is gratefully acknowledged. J.A.P. is supported by an Emma and Leslie Reid Scholarship from the University of Leeds.

Received: December 4, 2009
Revised: January 8, 2010
Accepted: January 11, 2010
Published online: February 11, 2010

Web Resources

The URLs for data presented herein are as follows:

Clustal W, http://www.ebi.ac.uk/clustalw2/
NCBI protein database, http://www.ncbi.nlm.nih.gov/protein
Online Mendelian Inheritance in Man (OMIM), http://www.ncbi.nlm.nih.gov/Omim/

References

1. Criswick, V.G., and Schepens, C.L. (1969). Familial exudative vitreoretinopathy. Am. J. Ophthalmol. *68*, 578–594.
2. Benson, W.E. (1995). Familial exudative vitreoretinopathy. Trans. Am. Ophthalmol. Soc. *93*, 473–521.
3. Chen, Z.Y., Battinelli, E.M., Fielder, A., Bundey, S., Sims, K., Breakefield, X.O., and Craig, I.W. (1993). A mutation in the Norrie disease gene (*NDP*) associated with X-linked familial exudative vitreoretinopathy. Nat. Genet. *5*, 180–183.
4. Robitaille, J., MacDonald, M.L.E., Kaykas, A., Sheldahi, L.C., Zeisler, J., Dube, M.P., Zhang, L.H., Singaraja, R.R., Guernsey, D.L., Zheng, B., et al. (2002). Mutant Frizzled-4 disrupts retinal angiogenesis in familial exudative vitreoretinopathy. Nat. Genet. *32*, 326–330.
5. Toomes, C., Bottomley, H.M., Jackson, R.M., Towns, K.V., Scott, S., Mackey, D.A., Craig, J.E., Jiang, L., Yang, Z., Trembath, R., et al. (2004). Mutations in *LRP5* or *FZD4* underlie the common familial exudative vitreoretinopathy locus on chromosome 11q. Am. J. Hum. Genet. *74*, 721–730.
6. Jiao, X., Ventruto, V., Trese, M.T., Shastry, B.S., and Hejtmancik, J.F. (2004). Autosomal recessive familial exudative vitreoretinopathy is associated with mutations in LRP5. Am. J. Hum. Genet. *75*, 878–884.
7. Kondo, H., Hayashi, H., Oshima, K., Tahira, T., and Hayashi, K. (2003). Frizzled 4 Gene (*FZD4*) mutations in patients with familial exudative vitreoretinopathy with variable expressivity. Br. J. Ophthalmol. *87*, 1291–1295.
8. Toomes, C., Bottomley, H.M., Scott, S., Mackey, D.A., Craig, J.E., Appukuttan, B., Stout, J.T., Flaxel, C.J., Zhang, K., Black, G.C., et al. (2004). Spectrum and frequency of FZD4 mutations in familial exudative vitreoretinopathy. Invest. Ophthalmol. Vis. Sci. *45*, 2083–2090.
9. Qin, M., Hayashi, H., Oshima, K., Tahira, T., Hayashi, K., and Kondo, H. (2005). Complexity of the genotype-phenotype correlation in familial exudative vitreoretinopathy with mutations in the LRP5 and/or FZD4 genes. Hum. Mutat. *26*, 104–112.
10. Nallathambi, J., Shukla, D., Rajendran, A., Namperumalsamy, P., Muthulakshmi, R., and Sundaresan, P. (2006). Identification of novel FZD4 mutations in Indian patients with familial exudative vitreoretinopathy. Mol. Vis. *12*, 1086–1092.
11. Kondo, H., Qin, M., Kusaka, S., Tahira, T., Hasebe, H., Hayashi, H., Uchio, E., and Hayashi, K. (2007). Novel mutations in Norrie disease gene in Japanese patients with Norrie disease and familial exudative vitreoretinopathy. Invest. Ophthalmol. Vis. Sci. *48*, 1276–1282.
12. Boonstra, F.N., van Nouhuys, C.E., Schuil, J., de Wijs, I.J., van der Donk, K.P., Nikopoulos, K., Mukhopadhyay, A., Scheffer, H., Tilanus, M.A., Cremers, F.P., and Hoefsloot, L.H. (2009). Clinical and molecular evaluation of probands and family members with familial exudative vitreoretinopathy. Invest. Ophthalmol. Vis. Sci. *50*, 4379–4385.
13. Downey, L.M., Keen, T.J., Roberts, E., Mansfield, D.C., Bamashmus, M., and Inglehearn, C.F. (2001). A new locus for autosomal dominant familial exudative vitreoretinopathy maps to chromosome 11p12-13. Am. J. Hum. Genet. *68*, 778–781.
14. Ye, X., Wang, Y., Cahill, H., Yu, M., Badea, T.C., Smallwood, P.M., Peachey, N.S., and Nathans, J. (2009). Norrin, frizzled-4, and Lrp5 signaling in endothelial cells controls a genetic program for retinal vascularization. Cell *139*, 285–298.
15. Clevers, H. (2009). Eyeing up new Wnt pathway players. Cell *139*, 227–229.
16. van Amerongen, R., and Nusse, R. (2009). Towards an integrated view of Wnt signaling in development. Development *136*, 3205–3214.
17. Berger, W., van de Pol, D., Bächner, D., Oerlemans, F., Winkens, H., Hameister, H., Wieringa, B., Hendriks, W., and Ropers, H.H. (1996). An animal model for Norrie disease (ND): gene targeting of the mouse ND gene. Hum. Mol. Genet. *5*, 51–59.
18. Wang, Y., Huso, D., Cahill, H., Ryugo, D., and Nathans, J. (2001). Progressive cerebellar, auditory, and esophageal dysfunction caused by targeted disruption of the frizzled-4 gene. J. Neurosci. *21*, 4761–4771.
19. Kato, M., Patel, M.S., Levasseur, R., Lobov, I., Chang, B.H., Glass, D.A. 2nd, Hartmann, C., Li, L., Hwang, T.H., Brayton, C.F., et al. (2002). Cbfa1-independent decrease in osteoblast proliferation, osteopenia, and persistent embryonic eye vascularization in mice deficient in Lrp5, a Wnt coreceptor. J. Cell Biol. *157*, 303–314.

20. Holmen, S.L., Giambernardi, T.A., Zylstra, C.R., Buckner-Berghuis, B.D., Resau, J.H., Hess, J.F., Glatt, V., Bouxsein, M.L., Ai, M., Warman, M.L., and Williams, B.O. (2004). Decreased BMD and limb deformities in mice carrying mutations in both Lrp5 and Lrp6. J. Bone Miner. Res. *19*, 2033–2040.
21. Xia, C.H., Liu, H., Cheung, D., Wang, M., Cheng, C., Du, X., Chang, B., Beutler, B., and Gong, X. (2008). A model for familial exudative vitreoretinopathy caused by LPR5 mutations. Hum. Mol. Genet. *17*, 1605–1612.
22. Xu, Q., Wang, Y., Dabdoub, A., Smallwood, P.M., Williams, J., Woods, C., Kelley, M.W., Jiang, L., Tasman, W., Zhang, K., and Nathans, J. (2004). Vascular development in the retina and inner ear: control by Norrin and Frizzled-4, a high-affinity ligand-receptor pair. Cell *116*, 883–895.
23. Luhmann, U.F., Lin, J., Acar, N., Lammel, S., Feil, S., Grimm, C., Seeliger, M.W., Hammes, H.P., and Berger, W. (2005). Role of the Norrie disease pseudoglioma gene in sprouting angiogenesis during development of the retinal vasculature. Invest. Ophthalmol. Vis. Sci. *46*, 3372–3382.
24. Junge, H.J., Yang, S., Burton, J.B., Paes, K., Shu, X., French, D.M., Costa, M., Rice, D.S., and Ye, W. (2009). TSPAN12 regulates retinal vascular development by promoting Norrin- but not Wnt-induced FZD4/beta-catenin signaling. Cell *139*, 299–311.
25. Ober, R.R., Bird, A.C., Hamilton, A.M., and Sehmi, K. (1980). Autosomal dominant exudative vitreoretinopathy. Br. J. Ophthalmol. *64*, 112–120.
26. Collins, J.S., and Schwartz, C.E. (2002). Detecting polymorphisms and mutations in candidate genes. Am. J. Hum. Genet. *71*, 1251–1252.
27. Henikoff, S., and Henikoff, J.G. (1992). Amino acid substitution matrices from protein blocks. Proc. Natl. Acad. Sci. USA *89*, 10915–10919.
28. Downey, L.M., Bottomley, H.M., Sheridan, E., Ahmed, M., Gilmour, D.F., Inglehearn, C.F., Reddy, A., Agrawal, A., Bradbury, J., and Toomes, C. (2006). Reduced bone mineral density and hyaloid vasculature remnants in a consanguineous recessive FEVR family with a mutation in LRP5. Br. J. Ophthalmol. *90*, 1163–1167.
29. Garcia-España, A., Chung, P.J., Sarkar, I.N., Stiner, E., Sun, T.T., and Desalle, R. (2008). Appearance of new tetraspanin genes during vertebrate evolution. Genomics *91*, 326–334.
30. Hemler, M.E. (2005). Tetraspanin functions and associated microdomains. Nat. Rev. Mol. Cell Biol. *6*, 801–811.
31. Stipp, C.S., Kolesnikova, T.V., and Hemler, M.E. (2003). Functional domains in tetraspanin proteins. Trends Biochem. Sci. *28*, 106–112.
32. Kovalenko, O.V., Metcalf, D.G., DeGrado, W.F., and Hemler, M.E. (2005). Structural organization and interactions of transmembrane domains in tetraspanin proteins. BMC Struct. Biol. *28*, 5:11.
33. Chenna, R., Sugawara, H., Koike, T., Lopez, R., Gibson, T.J., Higgins, D.G., and Thompson, J.D. (2003). Multiple sequence alignment with the Clustal series of programs. Nucleic Acids Res. *31*, 3497–3500.

Jpn J Ophthalmol 2010;54:622–637

LETTERS

A Case of Fukuyama Congenital Muscular Dystrophy Associated with Negative Electroretinograms

Fukuyama congenital muscular dystrophy (FCMD) is a congenital dystrophy associated with brain and eye abnormalities.[1] FCMD is an autosomal recessive disorder and occurs only in Japanese. Common ocular findings are optic atrophy, high myopia, cataracts, and weakness of the orbicularis muscles.[1] Abnormal vascular anastomosis and avascularization in the peripheral retina have also been reported. The eyes are only occasionally affected severely, for example, with retinal detachment and microphthalmia.

It was originally believed that patients with FCMD had normal electroretinograms (ERGs),[2] although a slight reduction of the b-wave and reduced ERGs under photopic conditions have been reported.[3,4] We describe an infant with FCMD exhibiting a severe form of ocular phenotype and negative-type ERG under dark-adapted conditions, a finding that to our knowledge has not been reported before.

Case Report

A 1-year-old boy had appeared normal at birth except for a right eye that was slightly microphthalmic. When he was 1 month old, a diagnosis of retinal detachment was made for the right eye (Fig. 1). His left eye was myopic with a tigroid appearance over the entire retina with pallor of the optic disc. The retinal vessels were tortuous, and the temporal peripheral retina was avascularized in both eyes. A scleral encircling buckle and subsequent vitrectomies were used to repair the retinal detachment in the right eye, but the retina remained detached. Before the surgery, the level of creatinine kinase was elevated (3634 IU/l), and the pediatrician suspected congenital muscular dystrophy despite the lack of any distinctive signs or a family history of muscular dystrophy.

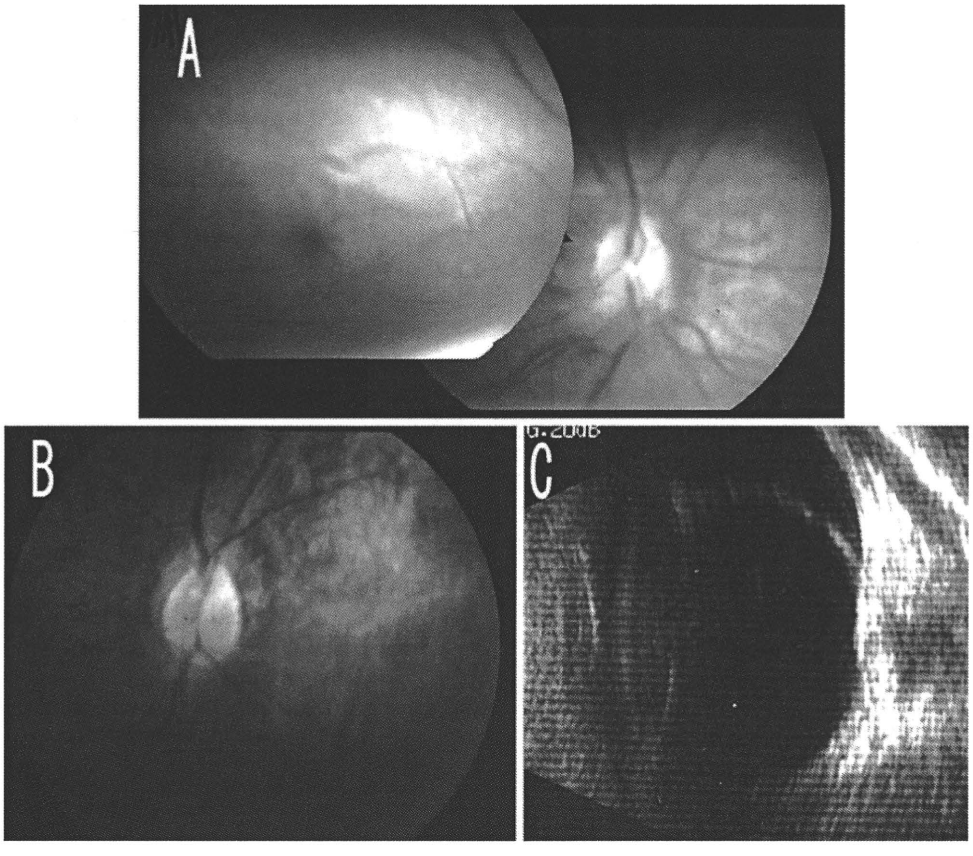

Figure 1A–C. Fundus photographs of our patient with Fukuyama congenital muscular dystrophy (FCMD). **A** Fundus photograph of the right eye showing a temporal retinal detachment involving the macula. **B** Fundus photograph of the left eye showing myopic tigroid appearance with pallor of the optic disc. **C** Ultrasonography showing the retinal detachment in the right eye.

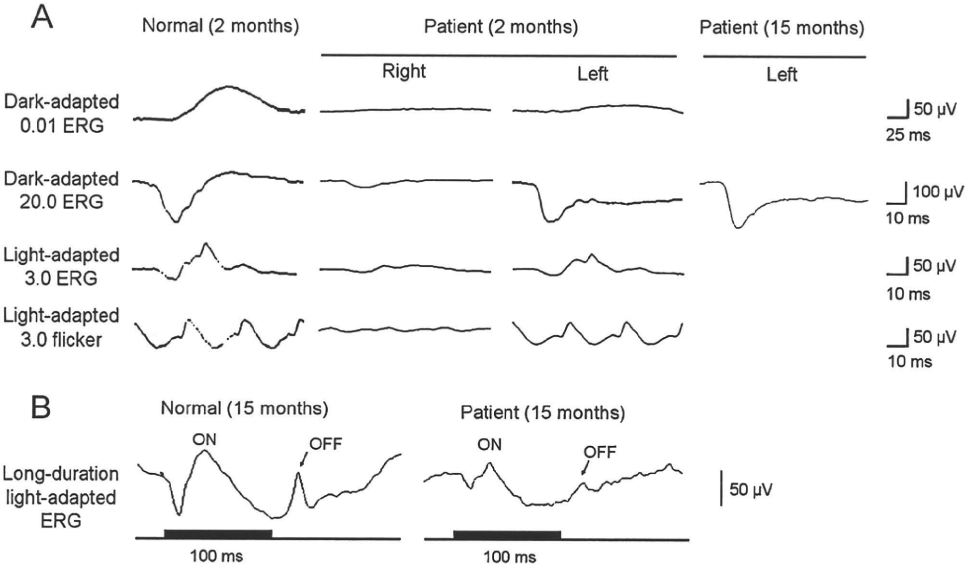

Figure 2A, B. Results of full-field electroretinograms (*ERGs*) using the International Society for Clinical Electrophysiology of Vision-recommended protocol recorded from our patient with FCMD. **A** ERGs recorded in a normal subject at age 2 months (left column), in our patient at 2 months (middle column), and in our patient at age 15 months. The amplitudes of the single-flash cone ERG and 30-Hz flicker ERGs were reduced but better preserved than the rod responses. Note that the maximum rod–cone response (dark-adapted, 20.0 ERG) of our patient showed a "negative" ERG waveform. **B** Light-adapted ERGs elicited by long-duration stimuli in a normal subject at age 15 months (*left*) and in our patient at age 15 months (*right*). Both the ON- and OFF-responses are equally reduced in our patient.

At 5 months, the patient was noted to have muscular weakness and was diagnosed with FCMD. The parents requested genetic testing to confirm the diagnosis. The patient was found to have compound heterozygous mutations in the *FKTN* gene; an insertion mutation in the 3′ noncoding region, and a point mutation, 250C- > T (R47X), in exon 3. The parents were found to be asymptomatic carriers.

During the first vitrectomy under general anesthesia, full-field ERGs were recorded using International Society for Clinical Electrophysiology of Vision-recommended standards (Fig. 2). Because of the retinal detachment, all ERG components in his right eye were severely attenuated. In his left eye, the rod response was decreased to about one-fifth of normal. The a-wave amplitude of the mixed rod–cone ERG was within normal limits, but the b-wave amplitude was smaller than the a-wave amplitude, indicating a negative-type ERG.

Comments

A negative ERG recorded under dark-adapted conditions has not been reported in patients with FCMD and therefore may be a new indication of FCMD. A compound heterozygous mutation in the *FKTN* gene, which occurs infrequently, is most likely the cause of the clinically severe phenotype. This negative-type ERG may be attributable to this less frequent genotype. A similar selective reduction of the b wave was described in patients with muscular dystrophies associated with changes in dystroglycan and dystrophin. The origin of the selective reduction is believed to be a disturbed neurotransmission from the photoreceptors to the ON-bipolar cells.[2]

To determine whether this negative-type ERG was caused by selective impairment of the postsynaptic ON-pathway, we also recorded light-adapted ERGs elicited by long-duration stimuli when our patient was 15 months old. We found that both the ON- and OFF-responses were equally reduced (Fig. 2B). This result is not in accord with the idea that the ON-bipolar cells are selectively disturbed, but an alternative possibility remains that the Müller cells or other neural elements are responsible for the reduction of the b wave because they are also believed to be involved in the generation of the b wave of ERGs.[5]

Acknowledgments. The authors thank Professor Akihiko Tawara for his critical comments and the patient and his parents for their cooperation. This work was partially supported by a Health and Labour Sciences Research Grant (20B-1) for Nervous and Mental Disorders and by Health and Labour Sciences Research Grants for Research on Intractable Diseases from the Ministry of Health, Labour and Welfare of Japan, and by Grants-in-Aid 19592047 and 22591956 for Scientific Research (C) from the Japan Society for the Promotion of Science.

Keywords: *FKTN*, Fukuyama congenital muscular dystrophy, microphthalmia, negative ERG, retinal detachment

Jpn J Ophthalmol
Vol 54: 622–637, 2010

Hiroyuki Kondo[1,2], Kayoko Saito[3], Mari Urano[3], Yukiko Sagara[3], Eiichi Uchio[2], and Mineo Kondo[4]
[1]Department of Ophthalmology, University of Occupational and Environmental Health, Japan, Kitakyushu, Japan; [2]Department of Ophthalmology, Fukuoka University School of Medicine, Fukuoka, Japan; [3]Institute of Medical Genetics, Tokyo Women's Medical University, Tokyo, Japan; [4]Department of Ophthalmology, Nagoya University Graduate School of Medicine, Nagoya, Japan

Received: February 24, 2010 / Accepted: June 29, 2010
Correspondence to: Hiroyuki Kondo, Department of Ophthalmology, University of Occupational and Environmental Health, Japan, 1-1 Iseigaoka, Yahatanishi-ku, Kitakyushu 807-8555, Japan
e-mail: kondohi@med.uoeh-u.ac.jp

DOI 10.1007/s10384-010-0875-0

References

1. Fukuyama Y, Osawa M, Suzuki H. Congenital progressive muscular dystrophy of the Fukuyama type—clinical, genetic and pathological considerations. Brain Dev 1981;3:1–29.
2. Santavuori P, Somer H, Sainio K, et al. Muscle-eye-brain disease (MEB). Brain Dev 1989;11:147–153.
3. Chijiiwa T, Nishimura M, Inomata H, Yamana T, Narazaki O, Kurokawa T. Ocular manifestations of congenital muscular dystrophy (Fukuyama type). Ann Ophthalmol 1983;15:921–923, 926–928.
4. Mishima H, Hirata H, Ono H, Choshi K, Nishi Y, Fukuda K. A Fukuyama type of congenital muscular dystrophy associated with atypical gyrate atrophy of the choroid and retina. A case report. Acta Ophthalmol (Copenh) 1985;63:155–159.
5. Ueda H, Gohdo T, Ohno S. Beta-dystroglycan localization in the photoreceptor and Muller cells in the rat retina revealed by immunoelectron microscopy. J Histochem Cytochem 1998;46:185–191.

Case of a Japanese Patient with X-linked Ocular Albinism Associated with the *GPR143* Gene Mutation

Albinism is an inherited disorder characterized by a reduction or absence of melanin in the hair, skin, and eyes. Albinism can be divided into two broad categories: oculocutaneous albinism and ocular albinism.[1] X-linked ocular albinism (XLOA) is characterized by nystagmus, decreased visual acuity, strabismus, fundus hypopigmentation, macular hypoplasia, and iris hypopigmentation with translucency. It is caused by mutations in the G protein-coupled receptor 143 (*GPR143*) gene (OMIM 300808), originally referred to as the *OA1* gene, which is located at Xp22.32.[2] The fundus of female carriers has a mosaic pattern of pigmentation and depigmentation, which helps in diagnosing XLOA.

We report on a Japanese boy with XLOA whose hair and skin appeared to be hypopigmented, causing some of the referring doctors and his parents to be concerned that he was suffering from oculocutaneous albinism. We detected a *GPR143/OA1* gene mutation, making this the first report of this mutation in Japan.

Case Report

The patient was a 4-month-old boy who had been born by normal delivery with a birth weight of 3148 g. His parents noticed that both his irides were blue and his eye movements appeared abnormal from birth. They consulted a pediatrician, who suspected oculocutaneous albinism. The patient was referred to us when he was 4 months old.

No family history of albinism was reported. His hair was mostly light brown, and his skin color was fair for a Japanese individual. He showed pendular horizontal nystagmus but could follow a slowly moving target. His refraction was –0.50 D = cyl –2.00 D Ax 180° (OD) and –0.50 D = cyl –1.50 D Ax 180° (OS). Slit-lamp examination showed that both irides were light brown (Fig. 1A, B). Bilateral foveal hypoplasia was present, and the ocular fundus was albinotic (Fig. 1C, D). Because his mother's fundus showed a mosaic pattern in the midperiphery, XLOA was diagnosed (Fig. 1E, F). He was also seen by a pediatrician of the Hamamatsu University School of Medicine, who diagnosed oculocutaneous albinism rather than ocular albinism (Fig. 1G, H). Because of the discrepancy in diagnoses, his parents wanted the diagnosis confirmed so as to know whether his skin needed to be protected from ultraviolet exposure.

After genetic counseling, the parents agreed to a genetic examination of their child and of themselves. The molecular genetics study was approved by the Institutional Review Board for Human Genetics and Genomic Research of Hamamatsu University School of Medicine. Nine exons and the surrounding regions of the *GPR143* gene were amplified by polymerase chain reaction (PCR) and directly sequenced. A splice mutation at the junction between exon 5 and intron 5, c.658+1G>A, was detected in the patient (Fig. 2). A heterozygous mutation was detected in his mother, but not in his father. The polymorphisms c.251–135C>T and c.767+10C>G were also detected in the patient.

Comments

This is the first report of a Japanese XLOA patient with a *GPR143* mutation. Various types of mutations in *GPR143* have been identified in Caucasian and Chinese populations. The splice mutation c.658+1G>A that we described here has been previously reported.[3]

Most Japanese patients with XLOA have brown irides that show no translucency, nonalbinotic fundi with moderate pigmentation, and normal skin and hair color.[4] However, the iris in our patient was light brown and the fundus was albinotic. His hair color was mostly light brown, and his skin color was fair for a Japanese individual. The skin and hair pigmentation in Caucasians with ocular albinism can be in the normal range but is frequently lighter in color than that of their siblings without XLOA. Recently, a Chinese family with XLOA and a *GPR143* mutation was reported to have iris hyperpigmentation.[5] Although the amount of pigment

Jpn J Ophthalmol
Vol 54: 622–637, 2010

Hiroyuki Kondo[1,2], Kayoko Saito[3], Mari Urano[3], Yukiko Sagara[3], Eiichi Uchio[2], and Mineo Kondo[4]
[1] Department of Ophthalmology, University of Occupational and Environmental Health, Japan, Kitakyushu, Japan; [2] Department of Ophthalmology, Fukuoka University School of Medicine, Fukuoka, Japan; [3] Institute of Medical Genetics, Tokyo Women's Medical University, Tokyo, Japan; [4] Department of Ophthalmology, Nagoya University Graduate School of Medicine, Nagoya, Japan

Received: February 24, 2010 / Accepted: June 29, 2010
Correspondence to: Hiroyuki Kondo, Department of Ophthalmology, University of Occupational and Environmental Health, Japan, 1-1 Iseigaoka, Yahatanishi-ku, Kitakyushu 807-8555, Japan
e-mail: kondohi@med.uoeh-u.ac.jp

DOI 10.1007/s10384-010-0875-0

References

1. Fukuyama Y, Osawa M, Suzuki H. Congenital progressive muscular dystrophy of the Fukuyama type—clinical, genetic and pathological considerations. Brain Dev 1981;3:1–29.
2. Santavuori P, Somer H, Sainio K, et al. Muscle-eye-brain disease (MEB). Brain Dev 1989;11:147–153.
3. Chijiiwa T, Nishimura M, Inomata H, Yamana T, Narazaki O, Kurokawa T. Ocular manifestations of congenital muscular dystrophy (Fukuyama type). Ann Ophthalmol 1983;15:921–923, 926–928.
4. Mishima H, Hirata H, Ono H, Choshi K, Nishi Y, Fukuda K. A Fukuyama type of congenital muscular dystrophy associated with atypical gyrate atrophy of the choroid and retina. A case report. Acta Ophthalmol (Copenh) 1985;63:155–159.
5. Ueda H, Gohdo T, Ohno S. Beta-dystroglycan localization in the photoreceptor and Muller cells in the rat retina revealed by immunoelectron microscopy. J Histochem Cytochem 1998;46:185–191.

Case of a Japanese Patient with X-linked Ocular Albinism Associated with the *GPR143* Gene Mutation

Albinism is an inherited disorder characterized by a reduction or absence of melanin in the hair, skin, and eyes. Albinism can be divided into two broad categories: oculocutaneous albinism and ocular albinism.[1] X-linked ocular albinism (XLOA) is characterized by nystagmus, decreased visual acuity, strabismus, fundus hypopigmentation, macular hypoplasia, and iris hypopigmentation with translucency. It is caused by mutations in the G protein-coupled receptor 143 (*GPR143*) gene (OMIM 300808), originally referred to as the *OA1* gene, which is located at Xp22.32.[2] The fundus of female carriers has a mosaic pattern of pigmentation and depigmentation, which helps in diagnosing XLOA.

We report on a Japanese boy with XLOA whose hair and skin appeared to be hypopigmented, causing some of the referring doctors and his parents to be concerned that he was suffering from oculocutaneous albinism. We detected a *GPR143*/*OA1* gene mutation, making this the first report of this mutation in Japan.

Case Report

The patient was a 4-month-old boy who had been born by normal delivery with a birth weight of 3148 g. His parents noticed that both his irides were blue and his eye movements appeared abnormal from birth. They consulted a pediatrician, who suspected oculocutaneous albinism. The patient was referred to us when he was 4 months old.

No family history of albinism was reported. His hair was mostly light brown, and his skin color was fair for a Japanese individual. He showed pendular horizontal nystagmus but could follow a slowly moving target. His refraction was –0.50 D = cyl –2.00 D Ax 180° (OD) and –0.50 D = cyl –1.50 D Ax 180° (OS). Slit-lamp examination showed that both irides were light brown (Fig. 1A, B). Bilateral foveal hypoplasia was present, and the ocular fundus was albinotic (Fig. 1C, D). Because his mother's fundus showed a mosaic pattern in the midperiphery, XLOA was diagnosed (Fig. 1E, F). He was also seen by a pediatrician of the Hamamatsu University School of Medicine, who diagnosed oculocutaneous albinism rather than ocular albinism (Fig. 1G, H). Because of the discrepancy in diagnoses, his parents wanted the diagnosis confirmed so as to know whether his skin needed to be protected from ultraviolet exposure.

After genetic counseling, the parents agreed to a genetic examination of their child and of themselves. The molecular genetics study was approved by the Institutional Review Board for Human Genetics and Genomic Research of Hamamatsu University School of Medicine. Nine exons and the surrounding regions of the *GPR143* gene were amplified by polymerase chain reaction (PCR) and directly sequenced. A splice mutation at the junction between exon 5 and intron 5, c.658+1G>A, was detected in the patient (Fig. 2). A heterozygous mutation was detected in his mother, but not in his father. The polymorphisms c.251–135C>T and c.767+10C>G were also detected in the patient.

Comments

This is the first report of a Japanese XLOA patient with a *GPR143* mutation. Various types of mutations in *GPR143* have been identified in Caucasian and Chinese populations. The splice mutation c.658+1G>A that we described here has been previously reported.[3]

Most Japanese patients with XLOA have brown irides that show no translucency, nonalbinotic fundi with moderate pigmentation, and normal skin and hair color.[4] However, the iris in our patient was light brown and the fundus was albinotic. His hair color was mostly light brown, and his skin color was fair for a Japanese individual. The skin and hair pigmentation in Caucasians with ocular albinism can be in the normal range but is frequently lighter in color than that of their siblings without XLOA. Recently, a Chinese family with XLOA and a *GPR143* mutation was reported to have iris hyperpigmentation.[5] Although the amount of pigment

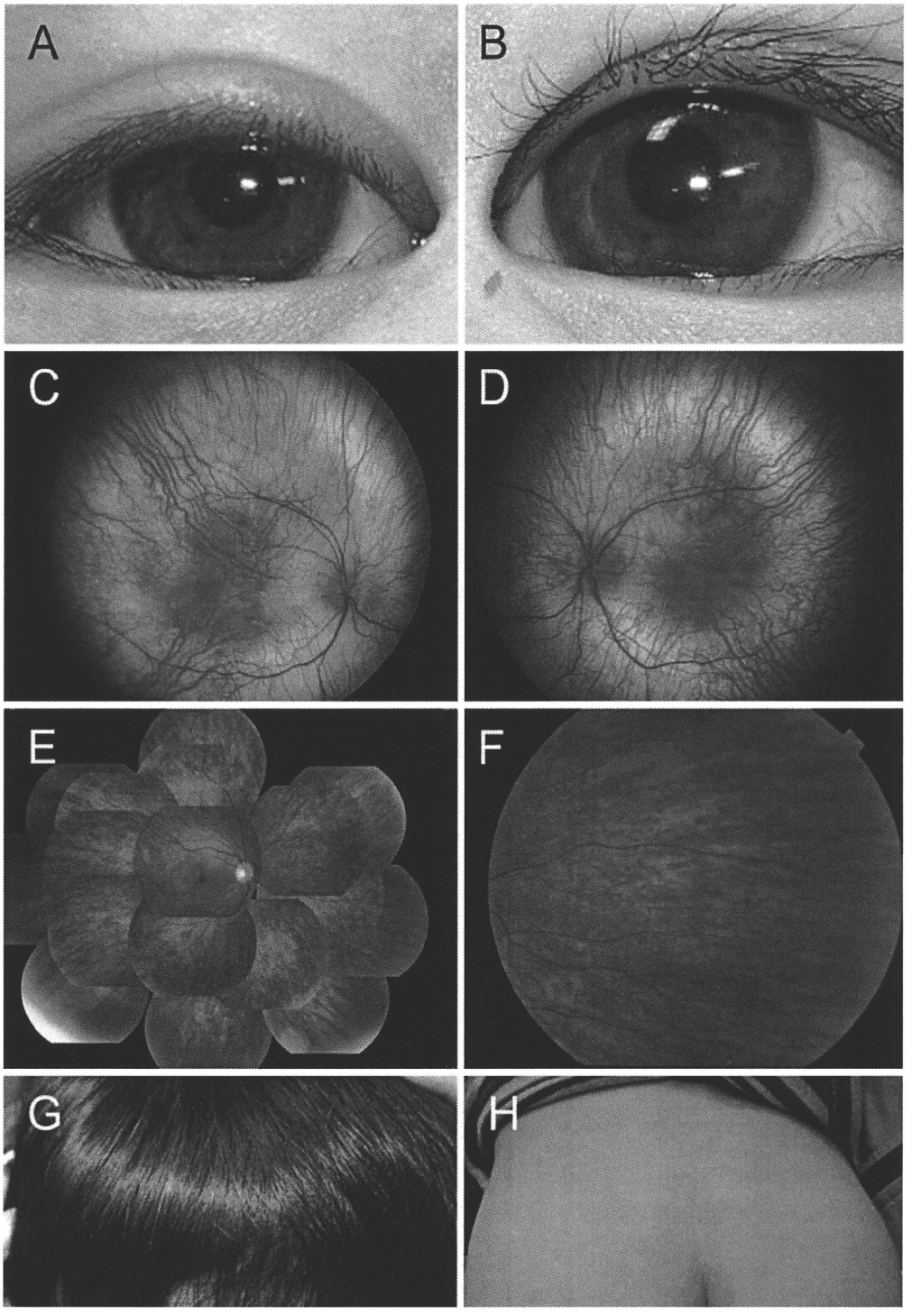

Figure 1. **A** Right eye, **B** left eye. Photos of irides taken when the patient was 18 months old. At the patient's birth, the irides were reported to be blue, but by 18 months they were light brown and without transillumination. **C** Right eye, **D** left eye. Fundus photographs taken at the first visit show an albinotic fundus. **E** Right eye, **F** left eye. Fundus photographs of the patient's mother (carrier) demonstrates sufficient pigment and a mosaic pattern at the midperiphery. **G** Photograph of the patient's hair taken when he was 18 months old. His hair color was light brown with some blond parts. **H** His skin color was fair for a Japanese person, and he had no Mongolian spots at birth.

Jpn J Ophthalmol
Vol 54: 622–637, 2010

in the iris and fundus in Asian patients appears to be between that of Caucasian and black patients, the phenotypic variations of XLOA vary considerably.

Keywords: *GPR143*, hypopigmentation, nystagmus, ocular albinism, skin

Masafumi Ohtsubo[1], Miho Sato[2], Akiko Hikoya[2], Katsuhiro Hosono[1,2], Shinsei Minoshima[1], and Yoshihiro Hotta[2]
[1]Department of Medical Photobiology, Photon Medical Research Center, Hamamatsu University School of Medicine, Hamamatsu, Japan; [2]Department of Ophthalmology, Hamamatsu University School of Medicine, Hamamatsu, Japan

Received: March 1, 2010 / Accepted: June 8, 2010
Correspondence to: Yoshihiro Hotta, Department of Ophthalmology, Hamamatsu University School of Medicine, 1-20-1 Handayama, Hamamatsu 431-3192, Japan
e-mail: hotta@hama-med.ac.jp

DOI 10.1007/s10384-010-0872-3

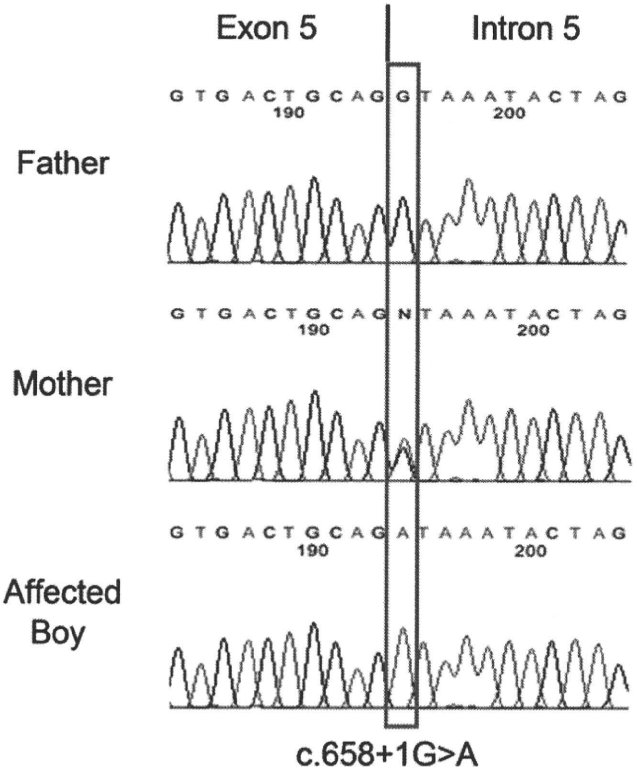

Figure 2. The patient had a splice mutation at the junction between exon 5 and intron 5 (G to A transition, c.658+1G > A) (*bottom*). A heterozygous mutation was detected in his mother (*middle*), but not in his father (*top*). The *box* indicates the position of the mutation, and the *vertical bar* over the box indicates the position of the exon–intron junction. Because the splice-donor site mutation tends to result in exon 5 being skipped, leading to a frameshift, the c.658+1G > A mutation can result in a truncated immature protein. This mutant protein is expected to lack transmembrane domain 5 and its following C-terminal side, including the G-protein binding region.

References

1. Kinnear PE, Jay B, Witkop CJ Jr. Albinism. Surv Ophthalmol 1985;30:75–101.
2. Bassi MT, Schiaffino MV, Renieri A, et al. Cloning of the gene for ocular albinism type 1 from the distal short arm of the X chromosome. Nat Genet 1995;10:13–19.
3. Fang S, Guo X, Jia X, Xiao X, Li S, Zhang Q. Novel *GPR143* mutations and clinical characteristics in six Chinese families with X-linked ocular albinism. Mol Vis 2008;14:1974–1982.
4. Shiono T, Tsunoda T, Chida Y, Nakazawa M, Tamai M. X linked ocular albinism in Japanese patients. Br J Ophthalmol 1995;79:139–143.
5. Xiao X, Zhang Q. Iris hyperpigmentation in a Chinese family with ocular albinism and the *GPR143* mutation. Am J Med Genet 2009;149A:1786–1788.

Congenital Toxoplasmosis Mimicking Microcephaly–Lymphedema–Chorioretinal Dysplasia

The combination of microcephaly, lymphedema, and chorioretinal dysplasia has been reported as a distinct hereditary entity (microcephaly–lymphedema–chorioreti-

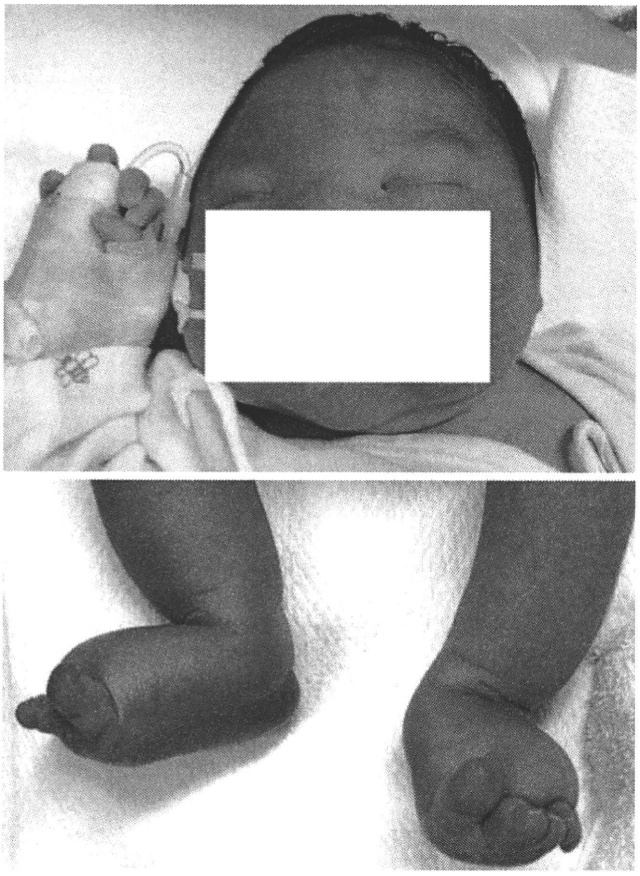

Figure 1. Microcephaly and marked lymphedema of dorsum of both feet.

Journal of Human Genetics (2010) 55, 701–703

www.nature.com/jhg

SHORT COMMUNICATION

Hair roots as an mRNA source for mutation analysis of Usher syndrome-causing genes

Hiroshi Nakanishi[1,2], Masafumi Ohtsubo[2], Satoshi Iwasaki[1], Yoshihiro Hotta[3], Kunihiro Mizuta[1], Hiroyuki Mineta[1] and Shinsei Minoshima[2]

mRNA is an important tool to study the effects of particular mutations on the mode of splicing and transcripts. However, it is often difficult to isolate mRNA because the organ or tissue in which the gene is expressed cannot be sampled. We previously identified two probable splicing mutations (c.6485+5G>A and c.8559-2A>G) during the mutation analysis of *USH2A* in Japanese Usher syndrome (USH) type 2 patients, but we could not observe their effects on splicing because the gene is expressed in only a few tissues/organs, and is not expressed in peripheral lymphocytes. In this study, we used hair roots as a source of mRNA of USH-causing genes, and successfully detected the expression of seven, except *USH1C* and *CLRN1*, of the nine USH-causing genes. We used RNA extracted from the hair roots of a patient who has both c.6485+5G>A and c.8559-2A>G mutations in *USH2A* in a compound heterozygous state to observe the effects of these mutations on transcripts. Reverse-transcription PCR analysis revealed that c.6485+5G>A and c.8559-2A>G inactivated splice donor and splice acceptor sites, respectively, and caused skipping of exons. Thus, RNA extracted from hair roots is a potential powerful and convenient tool for the mutation analysis of USH-causing genes.
Journal of Human Genetics (2010) **55,** 701–703; doi:10.1038/jhg.2010.83; published online 1 July 2010

Keywords: hair root; mRNA; Usher syndrome; *USH2A*

INTRODUCTION

To perform mutation analysis in the study of hereditary diseases, we generally used genomic DNA for the detection of mutations in exons and adjacent intronic regions of the gene of interest. Further, mRNA, if available, can also be used for the detection of mutations and for determining their effects on transcripts. However, except in the cases when the gene of interest is expressed in blood cells, it is difficult to isolate mRNA because the organ or tissue in which the gene of interest is expressed cannot be sampled.

We recently performed mutation analysis of *USH2A* gene for Japanese patients of Usher syndrome (USH) type 2, and identified 14 mutations, including 11 novel ones.[1] Of these mutations, two were splicing mutations, c.6485+5G>A and c.8559-2A>G in introns 33 and 42, respectively. We determined the pathogenicity of these mutations using supportive data, but could not examine their effect on pre-mRNA splicing because of the difficulty in obtaining *USH2A* mRNA. The expression of *USH2A* mRNA is restricted to a few tissues, including the retina and the cochlear, and is absent in peripheral lymphocytes.[2] Similarly, peripheral lymphocytes do not express mRNA of any other USH-causing genes, except *DFNB31*.[3]

Here, we attempted to use hair roots as a source of USH-causing gene mRNA. We successfully detected the mRNA expression of most USH-causing genes and analyzed the effect of the above-mentioned *USH2A* mutations on pre-mRNA splicing. This is the first report on the mRNA expression of USH-causing genes in hair roots.

MATERIALS AND METHODS

Collection of hair roots

At least 30 hair root samples were collected from the scalp of normal Japanese individuals and a USH type 2 patient. The patient had c.6485+5G>A and c.8559-2A>G mutations in *USH2A* in a compound heterozygous state (see the patient C152 in a previous report[1]). The institutional review board of Hamamatsu University School of Medicine approved this study, and written informed consent was obtained from all participants before enrollment.

Reverse-transcription PCR of USH-causing genes

Total RNA was extracted from the hair roots using the SV Total RNA Isolation System (Promega, Madison, WI, USA). Next, 2 μg of total RNA was reverse transcribed with oligo(dT) primers by using the SuperScript III First-Strand Synthesis System (Invitrogen, Carlsbad, CA, USA). Complementary DNA (cDNA) for all nine known USH-causing genes was amplified using specially designed PCR primers (Table 1). The PCR mixtures (total volume, 20 μl) contained 2 μg cDNA, 1.0 M betaine (Wako, Osaka, Japan), 1.5 mM $MgSO_4$, 0.3 μM each primer and 0.4 U KOD Plus DNA polymerase (Toyobo, Osaka, Japan). The amplification conditions were as follows: denaturation at 94 °C for

[1]Department of Otolaryngology, Hamamatsu University School of Medicine, Hamamatsu, Japan; [2]Department of Medical Photobiology, Photon Medical Research Center, Hamamatsu University School of Medicine, Hamamatsu, Japan and [3]Department of Ophthalmology, Hamamatsu University School of Medicine, Hamamatsu, Japan
Correspondence: Dr S Minoshima, Department of Medical Photobiology, Photon Medical Research Center, Hamamatsu University School of Medicine, 1-20-1 Handayama, Higashi-ku, Hamamatsu 431-3192, Japan.
E-mail: mino@hama-med.ac.jp
Received 20 March 2010; revised 1 June 2010; accepted 8 June 2010; published online 1 July 2010

Table 1 Nucleotide primers designed for PCR and sequencing of Usher syndrome-causing genes

Template	*Primer sequences (5′ to 3′)*	*Exon*	*Annealing temperature (°C)*[a]	*Product length (bp)*
MYO7A cDNA	F: TGAGATTGGGGCAGGAGTTCGACG	2	68	428
	R: GATGATGCAGCACTGGTCTCGGCT	4		
USH1C cDNA	F: AGTGGCCCGAGAATTCCGGCATAA	1	64	359
	R: CTGCCTGACCGCCTTTGATGAGGT	4		
CDH23 cDNA	F: GGTCGGCTTTGCCCTTCCACTCTT	11	64	449
	R: GTCCCGTGTCCTTGTCCAGCGAGA	14		
PCDH15 cDNA	F: TGCCAAACACTCGTGATTGCCGTC	8	64	330
	R: GACCGGCAAAGGCAGGAAGAGGAT	11		
USH1G cDNA	F: CCCACTCTCTGGGCTGCCTACCAT	1	68	443
	R: GTGAGGCTGGAGAAGCTGAGGGTGT	2		
USH2A cDNA	F: TAACTGCTTGCACTTTGGCTGGCT	31	64	613
	R: GTTAGGGCCTCACTGGCCTCACTC	35		
USH2A cDNA	F: GTGGTGACAGTGCTGGAACCCGAT	41	64	563
	R: ACAGTCACTTCTCGGCTCGGTGTAA	44		
GPR98 cDNA	F: ACTCACCTTTTGGCTTGGTGGGCT	53	64	533
	R: AAAGCTTCCAGCCAGCCGGACTAC	56		
DFNB31 cDNA	F: CTGCGCGTCAACGACAAATCCCTG	1	64	371
	R: CCTGGGTCCACGCCAGTGATGTAA	3		
CLRN1 cDNA	F: GCAATCCCAGTGAGCATCCACGTC	2	64	368
	R: GGGAACTGAAATCCAGCAAGTCGT	3		

Abbreviations: F, forward; R, reverse.
[a]The amplification conditions were as follows: denaturation at 94 °C for 2 min; followed by 40 cycles of treatment at 98 °C for 10 s, 64 or 68 °C for 30 s (see this column), and 68 °C for 1 min; and final extension at 68 °C for 5 min.

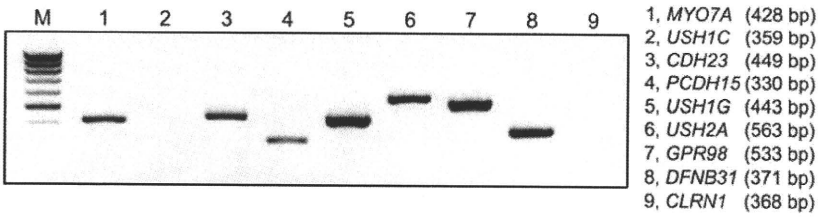

Figure 1 RT-PCR analysis of USH-causing genes. mRNA expression of all USH-causing genes, except *USH1C* and *CLRN1*, was detected in normal control hair roots. PCR was performed using 2 μg cDNA (total volume, 20 μl) with 40 cycles.

2 min; followed by 40 cycles of treatment at 98 °C for 10 s, 64 or 68 °C for 30 s (described in Table 1) and 68 °C for 2 min; and final extension at 68 °C for 5 min.

RESULTS

Detection of mRNA of USH-causing genes in hair roots

Total RNA was prepared from the scalp hair root samples obtained from normal individuals. Reverse-transcription PCR (RT-PCR) analysis revealed the mRNA expression of all USH-causing genes, except *USH1C* and *CLRN1*, in hair roots (Figure 1).

Detection of the splicing abnormality caused by *USH2A* splicing mutations

We next attempted to detect the splicing abnormality caused by the compound heterozygous mutations c.6485+5G>A and c.8559-2A>G in *USH2A*. Total RNA was prepared from the hair root samples obtained from the patient, and RT-PCR was performed using primers to amplify the cDNA between exons 31 and 35. Agarose gel electrophoresis of the RT-PCR products revealed two bands—a larger band corresponding to the normal sequence and a smaller band corresponding to the mutant sequence (Figure 2a). Sequence analysis of the mutants revealed that c.6485+5G>A causes skipping of exon 33 (160 bp) and presumably creates a premature stop codon in exon 34 through a frameshift. Similarly, RT-PCR performed using primers to amplify the cDNA between exons 41 and 44 revealed that c.8559-2A>G causes skipping of exon 43 (123 bp) (Figure 2b) and presumably induces a 41-amino-acid deletion. These results revealed that c.6485+5G>A and c.8559-2A>G inactivated splice donor and splice acceptor sites, respectively, and this finding confirmed the pathogenicity of these mutations.

DISCUSSION

RT-PCR analysis revealed the mRNA expression of seven of the nine USH-causing genes in hair roots. It has been reported that the mRNA of one USH-causing gene, *MYO7A* (causes USH type 1B), can be detected in the nasal epithelium;[4] however, obtaining *MYO7A* mRNA would necessitate invasive and painful tissue sampling methods. In contrast, collecting hair roots from the scalp is not an invasive procedure. Further, analysis of total RNA obtained from the hair roots of the patient with USH type 2 revealed that the two intronic mutations c.6485+5G>A and c.8559-2A>G inactivated a splice donor and splice acceptor sites, respectively, and both these mutations resulted in exon skipping. This is the first report to describe the RT-PCR analysis of *USH2A* mutations and show that the mutations close to the splice donor/acceptor sites cause splicing errors.

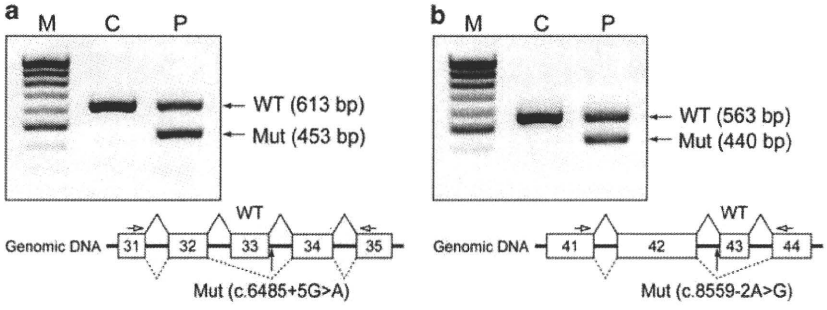

Figure 2 (**a**) Products of RT-PCR performed using primers to amplify *USH2A* cDNA between exons 31 and 35. The c.6485+5G>A mutation caused skipping of exon 33 (160 bp) and was presumed to create a premature stop codon in exon 34 through a frameshift. (**b**) Products of RT-PCR performed using primers to amplify *USH2A* cDNA between exons 41 and 44. The c.8559-2A>G mutation caused skipping of exon 43 (123 bp) and was presumed to create a 41-amino-acid deletion. Boxes with a number represent the exons. The solid and dotted lines that connect exons show the manner of splicing in the wild type and mutant, respectively. The distance between exons does not indicate the actual intron sizes. The open arrows indicate the PCR primers, and the closed arrows indicate mutations in introns. M, molecular marker (100 bp ladder); C, control; P, patient; WT, wild type; Mut, mutant.

Generally, mRNA is very useful for mutation analysis, especially in the case of coding-sequence mutations in large multi-exon genes, splicing mutations and regulatory-region mutations that affect the expression levels. Of these, the use of mRNA to determine the effect of a mutation on splicing as we revealed in this report is the most important advantage because we still cannot accurately predict splicing changes from DNA sequence alterations, especially if the alterations occur at a distance from splicing donor/acceptor sites[5] or within exonic splicing enhancers.[6]

Thus, mRNA extracted from hair roots is a potentially powerful and convenient tool for mutation analysis in USH-causing genes. Further, it is also reasonable to hypothesize that the mRNA of genes that cause deafness can be detected in hair roots, and this may facilitate easier and more accurate mutation analysis.

ACKNOWLEDGEMENTS

This work was supported by research grants from the Ministry of Health, Labour and Welfare (Acute Profound Deafness Research Committee), and from the Ministry of Education, Culture, Sports, Science and Technology (Young Scientists Grant B-20791189) in Japan.

1 Nakanishi, H., Ohtsubo, M., Iwasaki, S., Hotta, Y., Mizuta, K., Mineta, Y. *et al.* Identification of 11 novel mutations in USH2A among Japanese patients with Usher syndrome type 2. *Clin. Genet.* **76,** 383–391 (2009).
2 van Wijk, E., Pennings, R. J., te Brinke, H., Claassen, A., Yntema, H. G., Hoefsloot, L H. *et al.* Identification of 51 novel exons of the Usher syndrome type 2A (USH2A) gene that encode multiple conserved functional domains and that are mutated in patients with Usher syndrome type II. *Am. J. Hum. Genet.* **74,** 738–744 (2004).
3 Ebermann, I., Scholl, H. P., Charbel Issa, P., Becirovic, E., Lamprecht, J., Jurklies, B. *et al.* A novel gene for Usher syndrome type 2: mutations in the long isoform of whirlin are associated with retinitis pigmentosa and sensorineural hearing loss. *Hum. Genet.* **121,** 203–211 (2007).
4 Wolfrum, U., Liu, X., Schmitt, A., Udovichenko, I. P. & Williams, D. S. Myosin VIIa as a common component of cilia and microvilli. *Cell Motil. Cytoskeleton.* **40,** 261–271 (1998).
5 Nakai, K. & Sakamoto, H. Construction of a novel database containing aberrant splicing mutations of mammalian genes. *Gene.* **141,** 171–177 (1994).
6 Cartegni, L., Chew, S. L. & Krainer, A. R. Listening to silence and understanding nonsense: exonic mutations that affect splicing. *Nat. Rev. Genet.* **3,** 285–298 (2002).

Journal of Human Genetics (2010) 55, 796–800

www.nature.com/jhg

ORIGINAL ARTICLE

Mutation analysis of the *MYO7A* and *CDH23* genes in Japanese patients with Usher syndrome type 1

Hiroshi Nakanishi[1,2], Masafumi Ohtsubo[2], Satoshi Iwasaki[3], Yoshihiro Hotta[4], Yoshinori Takizawa[1], Katsuhiro Hosono[2,4], Kunihiro Mizuta[1], Hiroyuki Mineta[1] and Shinsei Minoshima[2]

Usher syndrome (USH) is an autosomal recessive disorder characterized by retinitis pigmentosa and hearing loss. USH type 1 (USH1), the second common type of USH, is frequently caused by *MYO7A* and *CDH23* mutations, accounting for 70–80% of the cases among various ethnicities, including Caucasians, Africans and Asians. However, there have been no reports of mutation analysis for any responsible genes for USH1 in Japanese patients. This study describes the first mutation analysis of *MYO7A* and *CDH23* in Japanese USH1 patients. Five mutations (three in *MYO7A* and two in *CDH23*) were identified in four of five unrelated patients. Of these mutations, two were novel. One of them, p.Tyr1942SerfsX23 in *CDH23*, was a large deletion causing the loss of 3 exons. This is the first large deletion to be found in *CDH23*. The incidence of the *MYO7A* and *CDH23* mutations in the study population was 80%, which is consistent with previous findings. Therefore, mutation screening for these genes is expected to be a highly sensitive method for diagnosing USH1 among the Japanese.
Journal of Human Genetics (2010) **55,** 796–800; doi:10.1038/jhg.2010.115; published online 16 September 2010

Keywords: *CDH23*; hearing loss; *MYO7A*; retinitis pigmentosa; Usher syndrome

INTRODUCTION

Usher syndrome (USH) is an autosomal recessive disorder characterized by retinitis pigmentosa (RP) and hearing loss (HL), with or without vestibular dysfunction.[1] It is the most common cause of combined deafness and blindness in industrialized countries, with a general prevalence of 3.5–6.2 per 100 000 live births.[2–7] The syndrome is clinically and genetically heterogeneous and can be classified into three clinical subtypes on the basis of the severity and progression of HL and the presence or absence of vestibular dysfunction.[8–10]

USH type 1 (USH1) is characterized by congenital severe-to-profound HL and vestibular dysfunction; it is the second common type after USH type 2 and accounts for 25–44% of the USH cases.[7,11] Five causative genes have been identified: myosin VIIA (HUGO gene symbol *MYO7A*); Usher syndrome 1C, harmonin (*USH1C*); cadherin-related 23 (*CDH23*); protocadherin-related 15 (*PCDH15*); and Usher syndrome 1G, Sans (*USH1G*).[12–18] Mutations in these genes have been observed in patients with USH1 from various ethnic origins, including Caucasian, African and Asian.[19] However, there have been no reports of mutation analysis for any responsible genes for USH1 in Japanese patients.

Of the five causative genes, the mutation frequency of *MYO7A* is the highest (39–55% of the total cases), followed by that of *CDH23* (19–35% of the total cases).[20,21] These two genes account for approximately 70–80% of the USH1 cases that have been analyzed.[20,21]

The aim of this study was to analyze mutations in the *MYO7A* and *CDH23* genes in Japanese patients with USH1.

MATERIALS AND METHODS

Subjects and diagnosis

Five unrelated Japanese patients (C103, C224, C312, C517 and C720) from various regions of Japan were referred to Hamamatsu University School of Medicine for genetic diagnosis of USH. All patients met the following criteria for USH1: RP, congenital severe-to-profound HL and vestibular dysfunction.[8] The clinical evaluation of the affected patients consisted of elicitation of the medical history, and ophthalmological and audiovestibular examinations. The medical history included the age at onset of walking, age at diagnosis of HL, nature of HL and age at diagnosis of RP.

The ophthalmological evaluation consisted of best-corrected visual acuity measurement, slit-lamp microscopy, ophthalmoscopy, Goldmann perimetry and electroretinography. Visual fields were evaluated by Goldmann perimetry of both eyes, and the isopters for the V/4e, III/4e and I/4e test targets were measured. Electroretinography was performed according to the International Society for Clinical Electrophysiology of Vision protocol.[22]

The auditory examination consisted of otoscopy, pure-tone audiometry (125–8000 Hz) and tympanometry. The severity of HL was classified using the pure-tone average over 500, 1000, 2000 and 4000 Hz in the better hearing ear as follows: normal hearing, <20 dB; mild HL, 21–40 dB; moderate HL, 41–70 dB; severe HL, 71–90 dB; and profound HL, >91 dB.

Vestibular function was evaluated on the basis of the medical history concerning childhood motor development and the results of caloric tests.

[1]Department of Otolaryngology, Hamamatsu University School of Medicine, Hamamatsu, Japan; [2]Department of Medical Photobiology, Photon Medical Research Center, Hamamatsu University School of Medicine, Hamamatsu, Japan; [3]Department of Hearing Implant Sciences, Shinshu University School of Medicine, Matsumoto, Japan and [4]Department of Ophthalmology, Hamamatsu University School of Medicine, Hamamatsu, Japan
Correspondence: Dr S Minoshima, Department of Medical Photobiology, Photon Medical Research Center, Hamamatsu University School of Medicine, 1-20-1 Handayama, Higashi-ku, Hamamatsu 431-3192, Japan.
E-mail: mino@hama-med.ac.jp
Received 10 July 2010; revised 16 August 2010; accepted 18 August 2010; published online 16 September 2010

Caloric stimulation of each ear was performed with cold water (20 °C, 5 ml) and the results were classified according to the peak slow-phase velocity as follows: normal, ⩾20°/s; canal paresis, <20°/s.[23] For the patient diagnosed with canal paresis, stronger stimulation with iced water (4 °C, 5 ml) was used to determine the presence of a residual response.

For all patients, parent samples were obtained for segregation analysis. A set of 135 control subjects, selected from Japanese individuals with no visual or hearing impairment, was used to assess the frequency of nucleotide sequence variations. The institutional review board of Hamamatsu University School of Medicine approved this study, and written informed consent was obtained from all subjects before enrollment.

Mutation analysis

Genomic DNA was extracted from peripheral lymphocytes by using standard procedures. In brief, the DNA samples were first screened for mutations in *MYO7A*, and the negative cases were screened for *CDH23* mutations. All exons (*MYO7A*, 49 exons; *CDH23*, 69 exons) and their flanking sequences were amplified by PCR. The PCR products were purified with Wizard SV Gel and PCR Clean-Up System (Promega, Madison, WI, USA) or treated with Exonuclease I and Antarctic Phosphatase (New England Biolabs, Ipswich, MA, USA). Direct sequencing was performed using the BigDye Terminator version 3.1 Cycle Sequencing Kit on an ABI 3100 Autosequencer (Applied Biosystems, Foster City, CA, USA). PCR amplification of *MYO7A* was performed using the primers described by Kumar *et al.*[24] with a slight modification. The PCR primers for *CDH23* amplification were newly designed. Information of the nucleotide sequence and appropriate annealing condition of all primers for PCR and sequencing is available on request. Using direct sequencing or restriction enzyme-based assay, we tested the Japanese control chromosomes for all the novel mutations identified during the mutation analysis.

Reverse-transcription PCR of *CDH23*

Reverse-transcription PCR (RT–PCR) of *CDH23* was preformed using total RNA extracted from hair roots as described previously.[25] The PCR primers were newly designed: forward primer, GCTTTTGGTGCTGATCTCTGGATGC located in exon 1; reverse primer, TGGTCGCTGACAGAGAACTCCACG in exon 4. The amplification condition was as follows: denaturation at 94 °C for 2 min; 40 cycles of treatment at 98 °C for 10 s, 64 °C for 30 s and 68 °C for 1 min; and final extension at 68 °C for 5 min.

RESULTS

Mutation analysis

Mutation analysis of *MYO7A* and *CDH23* in the five unrelated Japanese patients revealed five probable pathogenic mutations in four patients (Tables 1 and 2; Figure 1). Of these, two mutations (p.Tyr1942SerfsX23 in *CDH23* and p.Ala771Ser in *MYO7A*) were novel (Table 2). The former was a large deletion affecting 3 exons (Figure 2). The mutation was found in a homozygous state, which is probably accounted by consanguinity (Supplementary Figure 1). As the deletion caused the loss of 3 exons, resulted in a frameshift generating a premature stop codon at 23-codon downstream and was not identified in 64 control chromosomes, it was considered

Table 1 Clinical information of patients with probable pathogenic mutations

Patient	Age	Sex	Responsible gene	Mutations		Age[a]			Visual acuity		Visual field	ERG	Fundus of the eye	Cataract	Severity of HL	Caloric test
				Allele 1	Allele 2	Walking	HL	RP	Right	Left						
Homozygotes[b]																
C517	26	M	*CDH23*	p.Tyr1942 SerfsX23	p.Tyr1942 SerfsX23	22	2	3	0.1	0.1	5–10° with residual temporal field (V/4e)	Extinguished	Typical RP	No	Profound	CP
C720	13	F	*CDH23*	p.Arg2107X	p.Arg2107X	24	2	12	0.7	0.6	10–15° (V/4e)	Extinguished	Typical RP	No	Profound	CP
Compound heterozygotes																
C312	36	F	*MYO7A*	p.Arg150X	p.Arg1883Gln	24	2	10	0.5	0.7	5° (V/4e)	Extinguished	Typical RP	Both eyes	Profound	CP
Heterozygote																
C103	39	M	*MYO7A*	p.Ala771Ser	Unknown[c]	18	3	27	0.4	0.3	10–15° with residual temporal field (III/4e)	Extinguished	Typical RP	Both eyes	Profound	CP

Abbreviations: CP, canal paresis; ERG, electroretinography; HL, hearing loss; RP, retinitis pigmentosa.
[a]Age at onset of walking (months) and at diagnosis of HL and RP (years) are shown.
[b]The family of patient C517 has consanguinity (see Supplementary Figure 1), whereas that of patient C720 does not.
[c]The pathogenic allele remained undetected.

Table 2 Probable pathogenic mutations identified in the Japanese patients with USH1 examined in this study

Responsible gene	Nucleotide change	Predicted translation effect	Mutation type	Exon number	Domain[a]	Conservation in h/d/r/m/c/z species[b]	Number of alleles	Alleles in control chromosomes	Reference
CDH23	c.5821-?_6253+?del5078	p.Tyr1942SerfsX23	Deletion	44–46	EC18		2	0/64	This report
	c.6319C>T	p.Arg2107X	Nonsense	47	EC20		2	0/64	26
MYO7A	c.448C>T	p.Arg150X	Nonsense	5	Motor		1	0/64	12
	c.2311G>T	p.Ala771Ser	Missense	20	IQ	A/A/A/A/V/A	1	0/270	This report
	c.5648G>A	p.Arg1883Gln	Missense	41	MyTH4	R/R/R/R/R/R	1	0/200	21

[a]Detailed locations of the mutations are shown in Figure 1.
[b]h/d/r/m/c/z denote human/dog/rat/mouse/chicken/zebrafish myosin IIVa orthologs, respectively.

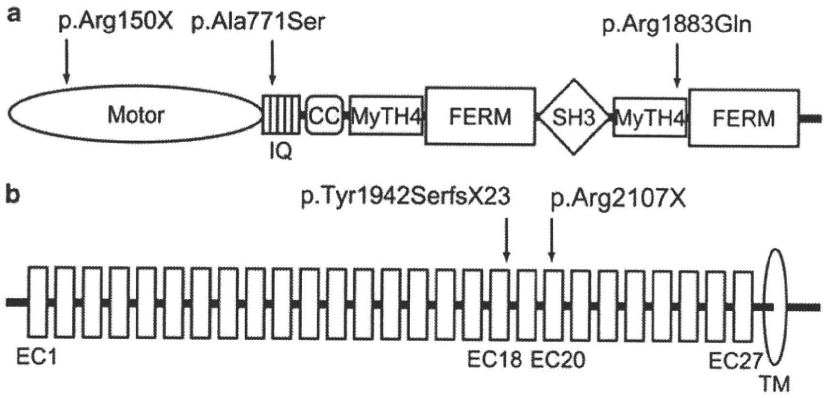

Figure 1 (**a**) Schema of myosin VIIa domains with mutations identified in *MYO7A*. The p.Arg150X, p.Ala771Ser and p.Arg1883Gln mutations were located in the Motor domain, IQ motif and MyTH4 domain, respectively. IQ, isoleucine-glutamine motif; CC, coiled-coil domain; MyTH4, myosin tail homology 4 domain; FERM, 4.1, ezrin, radixin, moesin domain; SH3, Src homology 3 domain. (**b**) Schema of cadherin 23 domains with mutations identified in *CDH23*. The p.Tyr1942SerfsX23 mutation changed Tyr1942 located in EC18 to Ser and created a premature stop codon at 23-codon downstream. The p.Arg2107X mutation was located in EC20. EC, extracellular domain; TM, transmembrane domain.

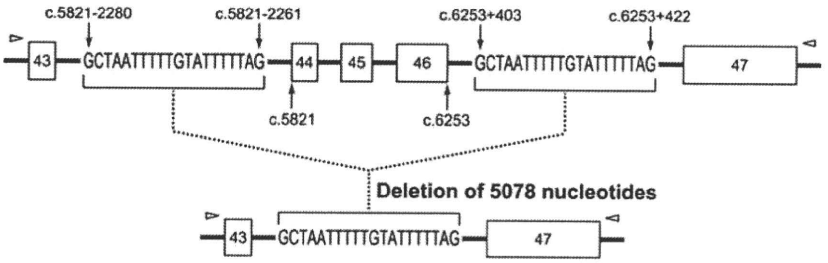

Figure 2 Schema of mutation p.Tyr1942SerfsX23 in the *CDH23* gene. The deletion occurred between introns 43 and 46, and both boundaries had 20-nucleotide sequence string GCTAATTTTTGTATTTTTAG. Upstream and downstream strings were located between c.5821-2280 and c.5821-2261 and between c.6253+403 and c.6253+422, respectively. Although the precise breakpoints could not be determined, the deletion size was elucidated to be 5078 nucleotides. The deletion was notated as c.5821-?_6253+?del5078. The boxes with a number represent exons. The distance between exons does not indicate the actual intronic sizes. The open arrowheads indicate the primer pairs used for PCR to amplify exons 43–47.

pathogenic. The other novel mutation (p.Ala771Ser in *MYO7A*) was considered pathogenic because it was not detected in 270 control chromosomes and Ala771 has been found to be almost conserved in various vertebrates (Table 2). Another mutation in patient C103 remained unclear. The remaining mutations (p.Arg150X and p.Arg1883Gln in *MYO7A*, and p.Arg2107X in *CDH23*) were previously reported and none of them was detected in the Japanese control chromosomes (Table 2).

In addition to the probable pathogenic mutations listed in Table 2, various sequence alterations were identified in *MYO7A* and *CDH23* (Table 3; Supplementary Tables 1 and 2). These alterations were predicted to be nonpathogenic for various reasons. Some of them have been reported as polymorphism in previous reports (Supplementary Tables 1 and 2). The newly identified alteration in exon 30 of *MYO7A* (p.Pro1261Pro) was also found in the control chromosomes. The newly found alterations in introns, except for c.68-3C>T in *CDH23* of patient C224, were distant from splicing donor or acceptor sites. The exception was not detected in any of the 270 control chromosomes but was considered benign because the RT–PCR analysis revealed that the alteration had no influence on splicing (Figure 3).

Table 3 Presumed nonpathogenic alterations that have never been reported

Nucleotide change	*Predicted translation effect*	*Exon/Intron number*	*Number of alleles*	*Alleles in control chromosomes*
Alterations in MYO7A among 5 patients (C103, C224, C312, C517 and C720)				
c.1691-125_126insT		Intron 14	5	
c.1797+55A>G		Intron 15	3	
c.3783C>T	p.Pro1261Pro	Exon 30	1	1/270
c.5944+57G>A		Intron 43	5	
c.5944+67C>T		Intron 43	5	
Alterations in CDH23 among 4 patients (C103, C224, C517 and C720)				
c.68-3C>T		Intron 1	1	0/270
c.3370-46T>C		Intron 27	4	
c.4206+61T>A		Intron 32	8	
c.4207-90G>A		Intron 32	4	
c.4489-98delA		Intron 35	3	

Clinical findings

All four patients in whom at least one mutant allele was detected had been diagnosed with RP by ophthalmologists at ages 3–27 years (mean ± s.d., 13.0 ± 10.1 years; Table 1). In all the patients, the visual fields were symmetrically constricted, pigmentary degeneration was typical of RP with peripheral bone-spicule pigmentation and standard combined electroretinography was extinguished. The best-corrected visual acuity ranged from 0.7 to 0.1. Two patients (C312 and C103) reported having cataracts, but none underwent cataract surgery.

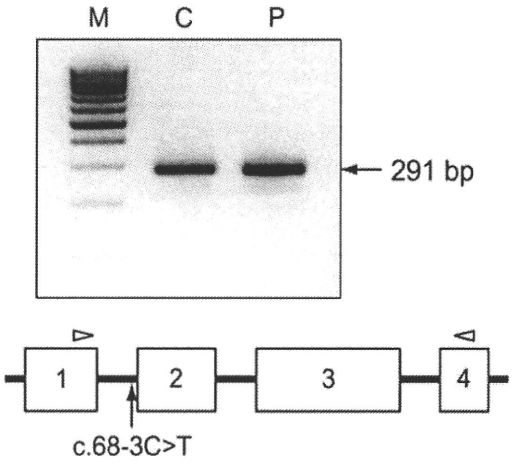

Figure 3 Products of reverse-transcription PCR (RT–PCR) performed using primers to amplify *CDH23* complementary DNA (cDNA) between exons 1 and 4. Agarose gel electrophoresis of the RT–PCR products revealed a single band with the proper size predicted from the normal sequence, indicating that the nucleotide change (c.68-3C>T) had no effect on splicing and was presumably nonpathogenic. PCR was performed using 2 μg cDNA (total volume, 20 μl) with 40 cycles. The boxes with a number represent exons. The distance between exons does not indicate the actual intronic sizes. The open arrowheads indicate the PCR primers, and the arrow indicates the nucleotide change. M, molecular marker (100-bp ladder); C, control; P, patient.

The patients were diagnosed with hearing impairment by otorhinolaryngologists at ages 2–3 years (2.3 ± 0.5 years; Table 1). Despite using hearing aids immediately after the diagnosis, all the patients did not develop speech ability and used sign language to communicate. Tympanometry yielded normal results, consistent with the clinical findings of a normal tympanic membrane and middle ear cavity. Audiograms showed bilateral profound sensorineural HL in all the patients. None of the patients complained of progressive HL.

All the patients reported delayed walking, with starting ages ranging from 18 to 24 months (22 ± 2.8 months; Table 1). The caloric test with cold water revealed canal paresis in all the patients, and no response was induced with the iced water. These results indicated that all the patients had congenital vestibular dysfunction.

DISCUSSION

This is the first report on mutation analysis of *MYO7A* and *CDH23* in Japanese patients with USH1. We found at least one mutant allele in four of the five patients in either of the genes. Although the number of patients examined was small, this frequency (80%) is similar to that among Caucasians, indicating that mutation screening for these genes is a highly sensitive method for diagnosing USH1 among the Japanese.

Of the five mutations identified in this study, three mutations (p.Arg150X and p.Arg1883Gln in *MYO7A*, and p.Arg2107X in *CDH23*) were previously identified in European-Caucasians.[12,21,26] All of these mutations occurred by transition (C/G→T/A) at CpG sites and were considered to be recurrent, which meets the fact that they are not specific to a particular ethnic group. This finding is consistent with a result of an analysis by Baux *et al.*,[27] who reported that a high proportion of *MYO7A* and *CDH23* mutations are represented by single base-pair substitutions and that 51.5 and 48.5% of them in *MYO7A* and *CDH23*, respectively, involve a CpG dinucleotide. Interestingly, neither of the two novel mutations found in the present study is of the transition type.

Mutation p.Tyr1942SerfsX23 (in *CDH23*) was found by PCR using a specially designed primer pair far distant from each other. After failing to amplify each of exons 44–46 in patient C517, we hypothesized the homozygous deletion of a long genomic region including at least exons 44–46. We successfully obtained an amplified product using a primer pair, one (forward) in intron 42 and the other (reverse) in intron 47 (Figure 2). Sequence analysis showed that the amplified DNA contains intact exon 43, truncated intron 43, truncated intron 46 and intact exon 47, indicating a deletion from introns 43 to 46. The boundary between truncated introns 43 and 46 had 20-nucleotide sequence string GCTAATTTTTGTATTTTTAG. Interestingly, the same 20-nucleotide sequences exist in normal introns 43 and 46, and lie within AluSx repetitive sequences. It is speculated that the deletion occurred with Alu-mediated recombination. We could not determine the precise breakpoints in both introns because of the exact sequence identity around possible breakpoints, but the deletion size was elucidated to be 5078 nucleotides regardless of the position of break. We notated the deletion as c.5821-?_6253+?del5078 according to a nomenclature guideline recommended by the Human Genome Variation Society (http://www.hgvs.org/mutnomen/).[28]

The deleted sequence in p.Tyr1942SerfsX23 included exons 44, 45 and 46 (103, 126 and 204 nucleotides long, respectively) and the total deletion size in mRNA was 433 nucleotides. Therefore, the mutation was presumed to create a premature stop codon at 23-codon downstream in exon 47 by a frameshift. This is the first large deletion to be found in *CDH23*. We could detect the mutation because of the loss of the same exons in both alleles by consanguinity. However, a large deletion of this type in only one allele cannot be easily detected by PCR because of the existence of the normal allele. In addition, we found a mutation p.Arg2107X in *CDH23* of patient C720. Both of these mutations are of a truncated type (nonsense, deletion/insertion with frameshift, or splicing). This finding is consistent with the previously reported genotype/phenotype relationship for *CDH23*: at least one of the two mutations is of a truncated type in USH1 cases, and both mutations are of a missense type in nonsyndromic HL cases.[29]

In conclusion, the mutation analysis of *MYO7A* and *CDH23* led to the identification of five mutations in four patients. This frequency (80%) indicates that mutation screening for these genes is a highly sensitive method for diagnosing USH1 among the Japanese. One novel mutation, p.Tyr1942SerfsX23 of *CDH23*, was a large deletion causing the loss of 3 exons: the homozygosity resulting from consanguinity probably led to the relatively easy identification. It is possible that similar exonal deletions latently exist in a compound heterozygous state in some USH1 cases in which only one mutation has been found.

ACKNOWLEDGEMENTS

We thank all the subjects who participated in the study. This work was supported by research grants from the Ministry of Health, Labour and Welfare (Acute Profound Deafness Research Committee) and the Ministry of Education, Culture, Sports, Science and Technology (Young Scientists Grant B-22791589) in Japan.

1 Yan, D. & Liu, X. Z. Genetics and pathological mechanisms of Usher syndrome. *J. Hum. Genet.* **55,** 327–335 (2010).
2 Nuutila, A. Dystrophia retinae pigmentosa—dysacusis syndrome (DRD): a study of the Usher or Hallgren syndrome. *J. Genet. Hum.* **18,** 57–88 (1970).
3 Boughman, J. A., Vernon, M. & Shaver, K. A. Usher syndrome: definition and estimate of prevalence from two high-risk populations. *J. Chronic Dis.* **36,** 595–603 (1983).
4 Grondahl, J. Estimation of prognosis and prevalence of retinitis pigmentosa and Usher syndrome in Norway. *Clin. Genet.* **31,** 255–264 (1987).

5 Hope, C. I., Bundey, S., Proops, D. & Fielder, A. R. Usher syndrome in the city of Birmingham: prevalence and clinical classification. *Br. J. Ophthalmol.* **81,** 46–53 (1997).
6 Rosenberg, T., Haim, M., Hauch, A- M. & Parving, A. The prevalence of Usher syndrome and other retinal dystrophy-hearing impairment associations. *Clin. Genet.* **51,** 314–321 (1997).
7 Spandau, U. H. & Rohrschneider, K. Prevalence and geographical distribution of Usher syndrome in Germany. *Graefes Arch. Clin. Exp. Ophthalmol.* **240,** 495–498 (2002).
8 Kimberling, W. J. & Möller, C. Clinical and molecular genetics of Usher syndrome. *J. Am. Acad. Audiol.* **6,** 63–72 (1995).
9 Tsilou, E. T., Rubin, B. I., Caruso, R. C., Reed, G. F., Pikus, A., Hejtmancik, J. F. *et al.* Usher syndrome clinical types I and II: could ocular symptoms and signs differentiate between the two types? *Acta Ophthalmol. Scand.* **80,** 196–201 (2002).
10 Pennings, R. J. E., Huygen, P. L. M., Orten, D. J., Wagenaar, M., van Aarem, A., Kremer, H. *et al.* Evaluation of visual impairment in Usher syndrome 1b and Usher syndrome 2a. *Acta Ophthalmol. Scand.* **82,** 131–139 (2004).
11 Grøndahl, J. & Mjøen, S. Usher syndrome in four Norwegian countries. *Clin. Genet.* **30,** 14–28 (1986).
12 Weil, D., Blanchard, S., Kaplan, J., Guilford, P., Gibson, F., Walsh, J. *et al.* Defective myosin VIIA gene responsible for Usher syndrome type 1B. *Nature* **374,** 60–61 (1995).
13 Bitner-Glindzicz, M., Lindley, K. J., Rutland, P., Blaydon, D., Smith, V. V., Milla, P. J. *et al.* A recessive contiguous gene deletion causing infantile hyperinsulinism, enteropathy and deafness identifies the Usher syndrome 1C gene. *Nat. Genet.* **26,** 56–60 (2000).
14 Verpy, E., Leibovici, M., Zwaenepoel, I., Liu, X. Z., Gal, A., Salem, N. *et al.* A defect in harmonin, a PDZ domain-containing protein expressed in the inner sensory hair cells, underlies Usher syndrome type 1C. *Nat. Genet.* **26,** 51–55 (2000).
15 Bolz, H., von Brederlow, B., Ramirez, A., Bryda, E. C., Kutsche, K., Nothwang, H. G. *et al.* Mutation of *CDH23,* encoding a new member of the cadherin gene family, causes Usher syndrome type 1D. *Nat. Genet.* **27,** 108–112 (2001).
16 Ahmed, Z. M., Riazuddin, S., Bernstein, S. L., Ahmed, Z., Khan, S., Griffith, A. J. *et al.* Mutations of the protocadherin gene PCDH23 cause Usher syndrome type 1F. *Am. J. Hum. Genet.* **69,** 25–34 (2001).
17 Alagramam, K. N., Yuan, H., Kuehn, M. H., Murcia, C. L., Wayne, S., Srisailpathy, C. *et al.* Mutations in the novel protocadherin PCDH15 cause Usher syndrome type 1F. *Hum. Mol. Genet.* **10,** 1709–1718 (2001).
18 Weil, D., El-Amraoui, A., Masmoudi, S., Mustapha, M., Kikkawa, Y., Laine, S. *et al.* Usher syndrome type IG (USH1G) is caused by mutations in the gene encoding SANS, a protein that associates with the USH1C protein, harmonin. *Hum. Mol. Genet.* **12,** 463–471 (2003).
19 Ahmed, Z. M., Riazuddin, S., Riazuddin, S. & Wilcox, E. R. The molecular genetics of Usher syndrome. *Clin. Genet.* **63,** 431–444 (2003).
20 Roux, A- F., Faugère, V., Le Guèdard, S., Pallares-Ruiz, N., Vielle, A., Chambert, S. *et al.* Survey of the frequency of USH1 gene mutations in a cohort of Usher patients shows the importance of cadherin 23 and protocadherin 15 genes and establishes a detection rate of above 90%. *J. Med. Genet.* **43,** 763–768 (2006).
21 Ouyang, X. M., Yan, D., Du, L. L., Hejtmancik, J. F., Jacobson, S. G., Nance, W. E. *et al.* Characterization of Usher syndrome type I gene mutations in an Usher syndrome patient population. *Hum. Genet.* **116,** 292–299 (2005).
22 Marmor, M. F., Holder, G. E., Seeliger, M. W. & Yamamoto, S. Standard for clinical electroretinography (2004 update). *Doc. Ophthalmol.* **108,** 107–114 (2004).
23 Nakanishi, H., Ohtsubo, M., Iwasaki, S., Hotta, Y., Mizuta, K., Mineta, H. *et al.* Identification of 11 novel mutations in USH2A among Japanese patients with Usher syndrome type 2. *Clin. Genet.* **76,** 383–391 (2009).
24 Kumar, A., Babu, M., Kimberling, W. J. & Venkatesh, C. P. Genetic analysis of a four generation Indian family with Usher syndrome: a novel insertion mutation in *MYO7A. Mol. Vis.* **10,** 910–916 (2004).
25 Nakanishi, H., Ohtsubo, M., Iwasaki, S., Hotta, Y., Mizuta, K., Mineta, H. *et al.* Hair roots as an mRNA source for mutation analysis of Usher syndrome-causing genes. *J. Hum. Genet.* **55,** 701–703 (2010).
26 Bork, J. M., Peters, L. M., Riazuddin, S., Bernstein, S. L., Ahmed, Z. M., Ness, S. L. *et al.* Usher syndrome 1D and nonsyndromic autosomal recessive deafness DFNB12 are caused by allelic mutations of the novel cadherin-like *CDH23. Am. J. Hum. Genet.* **68,** 26–37 (2001).
27 Baux, D., Faugère, V., Larrieu, L., Le Guèdard-Mèreuze, S., Hamroun, D., Bèroud, C. *et al.* UMD-USHbases: a comprehensive set of databases to record and analyse pathogenic mutations and unclassified variants in severe Usher syndrome causing genes. *Hum. Mutat.* **29,** E76–E87 (2008).
28 den Dunnen, J. T. & Antonarakis, S. E. Mutation nomenclature extensions and suggestions to describe complex mutations: a discussion. *Hum. Mutat.* **15,** 7–12 (2000).
29 Astuto, L. M., Bork, J. M., Weston, M. D., Askew, J. W., Fields, R. R., Orten, D. J. *et al. CDH23* mutation and phenotype heterogeneity: a profile of 107 diverse families with Usher syndrome and nonsyndromic deafness. *Am. J. Hum. Genet.* **71,** 262–275 (2002).

Supplementary Information accompanies the paper on Journal of Human Genetics website (http://www.nature.com/jhg)

あたらしい眼科 27(7)：869～874，2010

複視の画像診断

Imaging Diagnosis for Diplopia

西田保裕*

はじめに

複視は眼位，眼球運動の異常により生じ，その多くは後天性である．このため，複視を自覚する患者が来院した場合，まず原因を精査することが重要となる．その原因のなかには，眼窩内の外眼筋自体に病変が存在することがしばしばある．しかし，外眼筋は通常の眼科検査機器では観察できず，CT（コンピュータ断層撮影）やMRI（磁気共鳴画像）の画像診断が重要となり，その有用性が報告されている[1～6]．

本稿では，外眼筋の画像診断のために眼科医自らが適切なMRI検査のオーダーが行えるよう，撮像条件のポイントを具体的に解説する．さらに，代表的な外眼筋病変を呈示し，外眼筋画像診断でのMRIの有用性について述べたい．

I 外眼筋をMRIで観察する際の留意点

画像診断で外眼筋の形態観察をする場合の留意点は以下のとおりである．1）外眼筋の周囲は眼窩脂肪組織であるため，両組織に良好なコントラストが必要となる．2）外眼筋は1 cm^3 以下の小さい組織[2]であるため，関心領域の十分な絞り込みが必要となる．3）各外眼筋の走行は異なるため，各筋に応じたスライス方向の設定が必要となる．以上のようなことを留意し，MRIによる眼窩画像診断を行わなければならない．

II 眼窩MRIの具体的な条件設定

MRIは多くの種類の画像が得られる反面，その条件設定はCTに比較して複雑である．このため，外眼筋画像に適した条件を選択する必要がある．

1. 撮像法

MRIでは観察目的に応じて，さまざまな撮像法が考案されているが，スピンエコー法はMRIが臨床応用された当時から汎用されている基本的な撮像法である．図1のスピンエコー法のT1強調像（左写真）とT2強調像（右写真）では，眼窩内では高信号の脂肪組織の中に低から中等度信号の外眼筋が，高いコントラストで描出されている．また，T2強調像では硝子体・前房が白く描出されているように，水により高信号となるため，炎症による外眼筋浮腫の把握が可能となる．

一方，脂肪抑制画像の一つであるSTIR（short TI inversion recovery）法は，眼窩内で最も高い脂肪組織の信号を選択的に抑制する撮像法である．そして，脂肪組織以外の外眼筋，視神経の信号亢進を強調するSTIR法では図2の写真の矢印で示すように，炎症による外眼筋浮腫で信号強度が上昇する．ただし，脂肪抑制画像は外眼筋炎症の評価には非常に有用だが，外眼筋と脂肪組織のコントラストは低いため形態観察には不向きである．形態観察目的でオーダーしたはずのスピンエコー画像が，すべて脂肪抑制された画像で送られてくることも

*Yasuhiro Nishida：滋賀医科大学眼科学講座
〔別刷請求先〕西田保裕：〒520-2192 大津市瀬田月輪町　滋賀医科大学眼科学講座

0910-1810/10/¥100/頁/JCOPY